

## Supplementary tables and figures

### Topical application of TAK1 inhibitor encapsulated by gelatin particle alleviates corneal neovascularization

Jiang-Hui Wang<sup>1†</sup>, Ching-Li Tseng<sup>2†</sup>, Fan-Li Lin<sup>3,4</sup>, Jinying Chen<sup>5</sup>, Erh-Hsuan Hsieh<sup>2</sup>, Suraj Lama<sup>3</sup>, Yu-Fan Chuang<sup>3,4</sup>, Satheesh Kumar<sup>3</sup>, Linxin Zhu<sup>3</sup>, Myra B. McGuinness<sup>1,6</sup>, Jessika Hernandez<sup>3</sup>, Leilei Tu<sup>5</sup>, Peng-Yuan Wang<sup>4</sup>, Guei-Sheung Liu<sup>1,2,3,7,8\*</sup>

<sup>1</sup>Centre for Eye Research Australia, Royal Victorian Eye and Ear Hospital, East Melbourne, Australia

<sup>2</sup>Graduate Institute of Biomedical Materials and Tissue Engineering, College of Biomedical Engineering, Taipei Medical University, Taipei, Taiwan

<sup>3</sup>Menzies Institute for Medical Research, University of Tasmania, Hobart, Australia

<sup>4</sup>Shenzhen Key Laboratory of Biomimetic Materials and Cellular Immunomodulation, Shenzhen Institute of Advanced Technology, Chinese Academy of Sciences, Shenzhen, China

<sup>5</sup>Department of Ophthalmology, the First Affiliated Hospital of Jinan University, Guangzhou, China

<sup>6</sup>Centre for Epidemiology and Biostatistics, Melbourne School of Population and Global Health, University of Melbourne, Melbourne, Australia

<sup>7</sup>Ophthalmology, Department of Surgery, University of Melbourne, East Melbourne, Australia

<sup>8</sup>Aier Eye Institute, Changsha, Hunan, China

†JHW and CLT contributed equally to this work

\*Correspondence and requests for materials should be addressed to

Dr Guei-Sheung Liu (rickliu0817@gmail.com). Menzies Institute for Medical Research, University of Tasmania. Address: 17 Liverpool Street, Hobart, TAS 7000, Australia. Tel: +61362264250.

## Supplementary tables

**Table S1** Key Resources table

REAGENT or RESOURCE	SOURCE	IDENTIFIER
<b>Antibodies</b>		
I $\kappa$ B $\alpha$ (L35A5) mouse mAb	Cell Signaling Technology	4814
Phospho-NF $\kappa$ B p65 (Ser536) (93H1) rabbit mAb	Cell Signaling Technology	3033
NF $\kappa$ B p65 (C22B4) rabbit mAb	Cell Signaling Technology	4764
Phospho-p44/42 MAPK (Erk1/2) (Thr202/Tyr204) rabbit pAb	Cell Signaling Technology	9101
p44/42 MAPK (Erk1/2) (137F5) rabbit mAb	Cell Signaling Technology	4695
Phospho-SAPK/JNK (Thr183/Tyr185) (G9) mouse mAb	Cell Signaling Technology	9255
SAPK/JNK rabbit pAb	Cell Signaling Technology	9252
Phospho-p38 MAPK (Thr180/Tyr182) rabbit pAb	Cell Signaling Technology	9211
p38 MAPK (D13E1) XP <sup>®</sup> rabbit mAb	Cell Signaling Technology	8690
Actin (clone C4) mouse mAb	Merck Millipore	MAB1501
Goat anti-mouse IgG HRP-conjugated secondary Ab	Life Technologies Australia	31430
Goat anti-rabbit IgG HRP-conjugated secondary Ab	Life Technologies Australia	656120
<b>Chemicals</b>		
5Z-7-Oxozeaenol	Tocris Bioscience	3604/1
Recombinant Human TNF $\alpha$ protein	Gibco <sup>™</sup>	PHC3015
Recombinant Human VEGF165 Protein	R&D Systems	293-VE-010
Type A gelatin (bloom 175)	Sigma-Aldrich	G2625
DMSO	JT Baker	9224-01
Glutaraldehyde	Sigma-Aldrich	G6257
Acetone	Seedchem Company	AC0061
Uranium acetate	Thermo Fisher Scientific	541-09-3
Acetonitrile	Aencore Chemical	AE0627
5-Carboxytetramethylrhodamine, succinimidyl ester (5-TAMRA)	Thermo Fisher Scientific	C2211
Zoletil 50 <sup>®</sup>	Virbac	n/a
Rompun <sup>®</sup>	Bayer	n/a
Alcaine <sup>®</sup>	Alcon	n/a
Silver Nitrate Applicators 6 inch	Grafco	1590
DAPI	Generon	40043
<b>Critical Commercial Assays</b>		
CYQUANT <sup>®</sup> NF cell proliferation assay kit	Life Technologies	C35006

	Australia	
Quick-RNA MiniPrep kit	Zymo Research	R1055
High-capacity cDNA reverse transcription Kit	Life Technologies Australia	4368814
TaqMan™ Fast Advanced Master Mix	Life Technologies Australia	4444553
Pierce™ BCA assay kit	Life Technologies Australia	23227
Amersham ECL Prime Western Blotting Detection Kit	GE Healthcare	RPN2232
MycoAlert™ Mycoplasma Detection Kit	Lonza	LT07
<b>Experimental Models: Cell Lines</b>		
Telomerase-immortalized human microvascular endothelium cell (TIME)* *Cell was derived from a primary culture of neonatal foreskin microvascular endothelial cells of the dermis.	ATCC	CRL-4025™
Human Umbilical Vein Endothelial Cell (HUVEC)* *Cells was derived from the endothelium of veins from the umbilical cord.	Life Technologies Australia	C0035C
<b>Experimental Models: Organisms/Strains</b>		
C57BL/6 mouse	Taipei Medical University	LAC-2015-0328 and LAC-2019-063
<b>qPCR Probes</b>		
Human VEGFA TaqMan probe	Applied Biosystems	Hs00900055_m1
Human ICAM1 TaqMan probe	Applied Biosystems	Hs00164932_m1
Human PTGS2 TaqMan probe	Applied Biosystems	Hs00153133_m1
Human CXCL8 TaqMan probe	Applied Biosystems	Hs00174103_m1
Human GAPDH TaqMan probe	Applied Biosystems	Hs99999905_m1
Mouse TNFa TaqMan probe	Applied Biosystems	Mm00443258_m1
Mouse IL1b TaqMan probe	Applied Biosystems	Mm00434228_m1
Mouse actin-b TaqMan probe	Applied Biosystems	Mm00607939_s1
<b>Software and Algorithms</b>		
Image Pro Plus	Media Cybernetics	n/a
ImageJ (v1.48)	Schneider et al., 2012 <a href="https://imagej.nih.gov/ij">https://imagej.nih.gov/ij</a>	n/a
Adobe Photoshop	Adobe. Connor et al., 2009	n/a
GraphPad Prism 7	GraphPad Software	n/a
R (v4.0.2)	Bioconductor	n/a
Trimalore (v0.4.4)	Babraham Institute	n/a
STAR (v2.5.3)	Alexander Dobin	n/a
FeatureCounts (subread 1.6.4)	Liao Y, Smyth GK and Shi W., 2014	n/a
<b>Other</b>		
Matrigel™ Basement Membrane Matrix	Corning	356234
Pierce RIPA buffer	Life Technologies	89900

	Australia	
Protease inhibitor cocktail	Roche Diagnostics	11697498001
Bolt™ 4-12% Bis-Tris Plus Gel	Invitrogen	NW04120BOX
Immuno-Blot® PVDF Membrane	Bio-Rad Laboratories	1620177
EBM™ Plus Basal Medium supplied with EGM™ Plus SingleQuots™ supplements	Lonza	CC-5035
Modified Davidson's fluid	CIS-Bio, Taiwan	D476
10 % neutral buffered formalin solution	CIS-Bio, Taiwan	D468
FSC22 Frozen section media	Leica	3801480
Fluoromount™ aqueous mounting medium	Sigma-Aldrich	F-4680
Incucyte® 96-well WoundMaker Tool	Incucyte	4563
TrypLE Express Enzyme (1X)	Life Technologies Australia	12605028
Spectra/Por, Float-A-Lyzer G2 Dialysis Device (MWCO 20 kDa)	Sigma-Aldrich	Z726710-12EA

**Table S2** Estimated rate of change in fluorescent intensity from a piecewise linear mixed-effects model

	Dye	Average rate of change		Difference to free dye			Difference to first 10 mins		
		%/minute	(95% CI)	%/minute	(95% CI)	p-value*	%/minute	(95% CI)	p-value*
0-10 mins	Free dye	-5.4	(-6.2,-4.7)						
	TAMRA-GNPs	-4.5	(-5.2,-3.7)	0.9	(-0.1,2.0)	0.083			
	TAMRA-GNPs-Oxo	-0.8	(-1.6,-0.1)	4.6	(3.5,5.7)	<0.001			
>10-60 mins	Free dye	-0.7	(-1.1,-0.4)				4.7	(3.9,5.5)	<0.001
	TAMRA-GNPs	0.0	(-0.3,0.3)	0.7	(0.3,1.2)	0.002	4.5	(3.7,5.3)	<0.001
	TAMRA-GNPs-Oxo	-0.5	(-0.9,-0.2)	0.2	(-0.2,0.7)	0.380	0.3	(-0.5,1.1)	0.505

\* Derived from a piecewise linear mixed-effects model with random intercepts and slopes

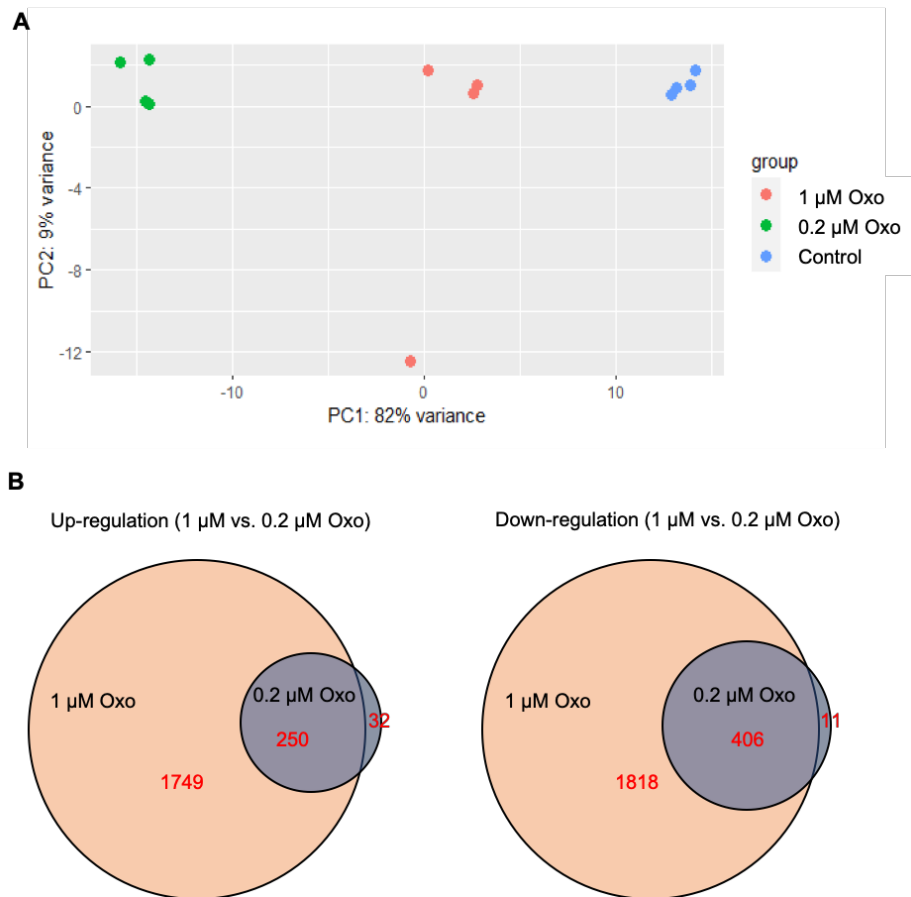
**Table S3** Observed values at specific time points from Figure 4F

Time	Dye	Fluorescent intensity (%)	Difference free dye (%)	
		Average (SD)	Average	p-value*
10 mins	Free dye	40.4 (13.1)		
	TAMRA-GNPs	57.1 (9.8)	16.7 (9.5)	0.153
	TAMRA-GNPs-Oxo	95.3 (6.9)	54.9 (8.5)	0.003
60 mins	Free dye	24.2 (5.4)		
	TAMRA-GNPs	54.1 (9.2)	29.9 (6.1)	0.008
	TAMRA-GNPs-Oxo	75.3 (24.4)	51.2 (14.4)	0.024

\* Derived from two sample t-tests

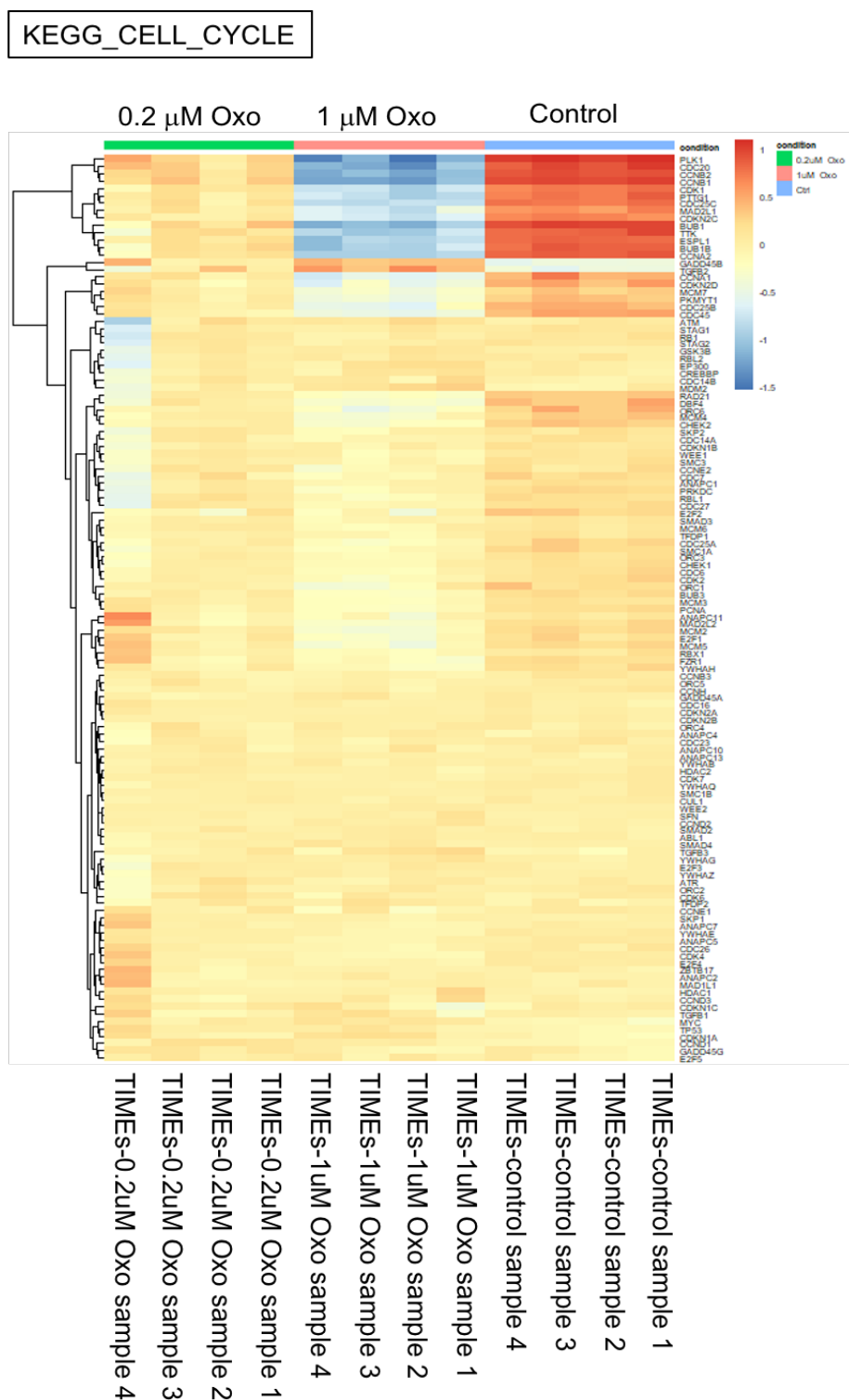
## Supplementary figures

Figure S1



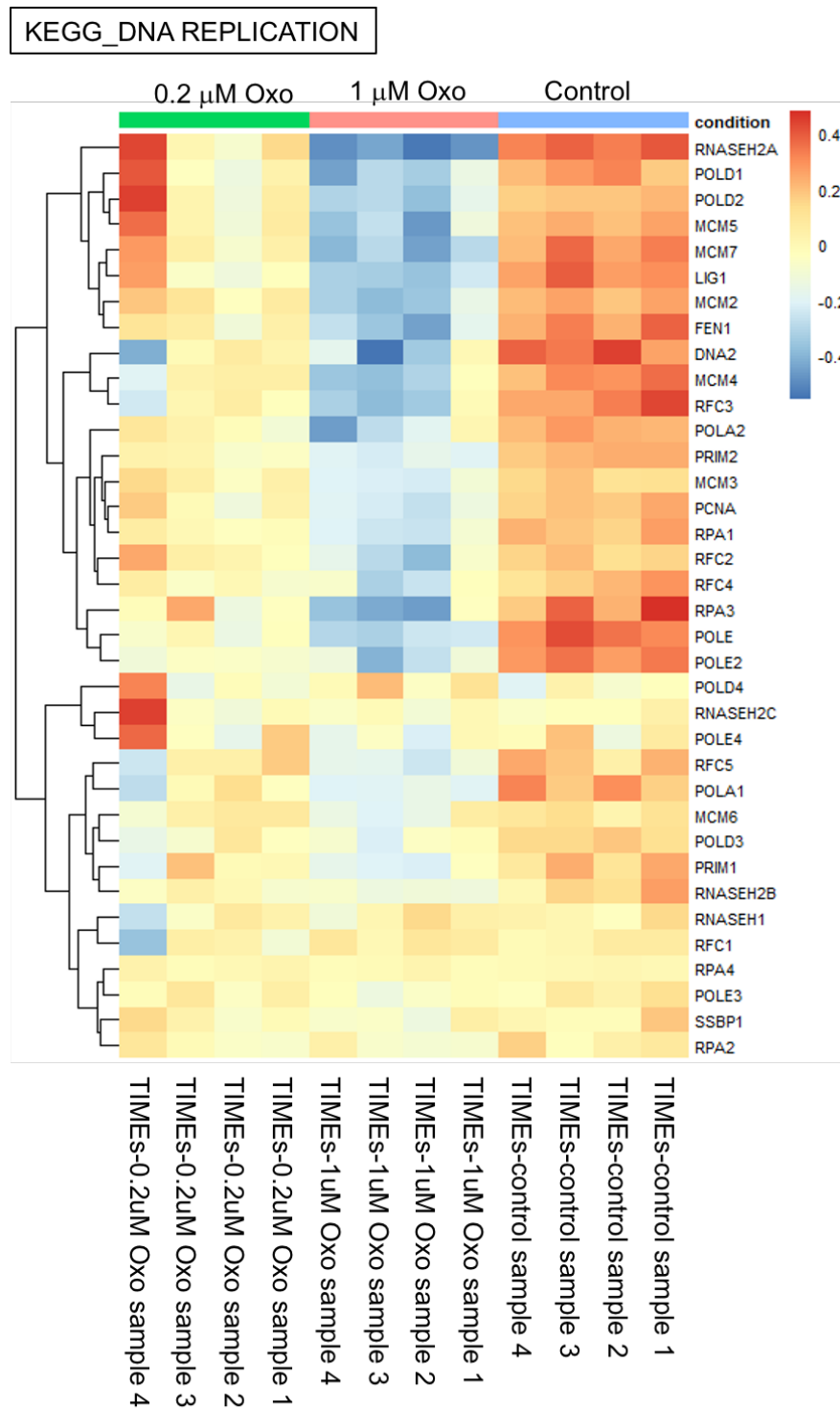
**Figure S1 (A)** Principal component analysis of RNA-seq data of control, 0.2  $\mu$ M and 1  $\mu$ M 5Z-7-oxozeaenol treated human telomerase-immortalized human microvascular endothelial (TIME) cells. Each dot represents an experimental replicate. **(B)** Venn diagram shows the overlapped dysregulated genes between dysregulated genes identified in 0.2  $\mu$ M and 1  $\mu$ M 5Z-7-oxozeaenol treated TIME cells.

Figure S2



**Figure S2** Heat map generated from unsupervised clustering of genes from gene set of ‘cell cycle’ (Reactome Pathway Database) of 0.2  $\mu$ M and 1  $\mu$ M 5Z-7-oxozeaenol treated TIME cells and normal controls.

Figure S3

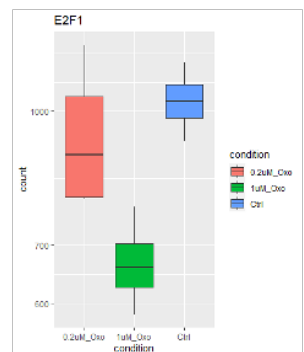
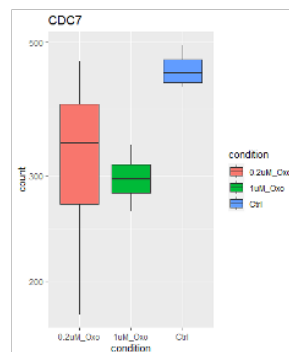
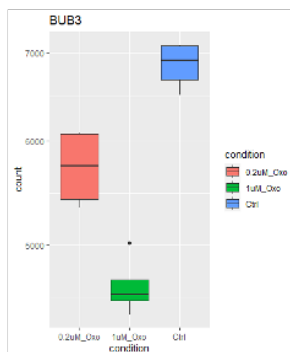
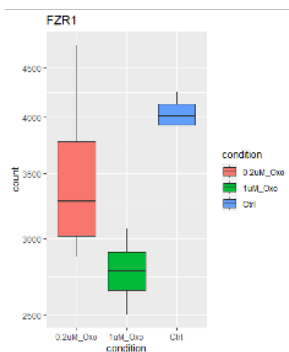
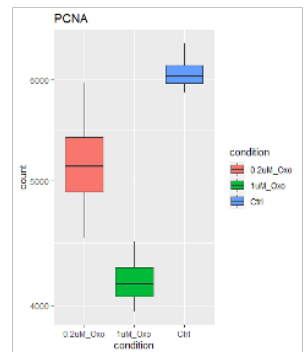
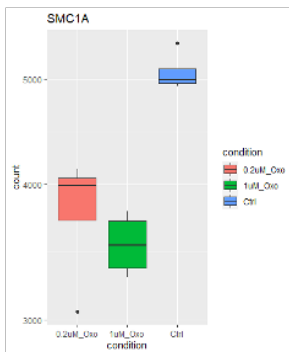
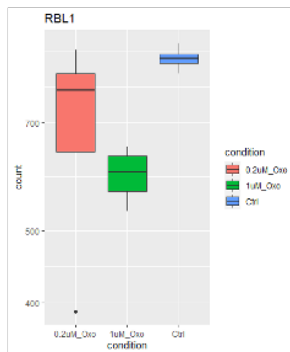
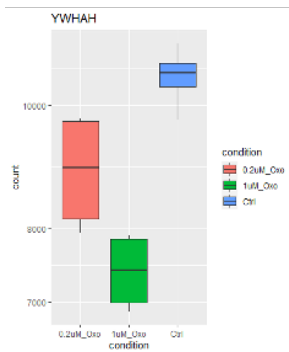
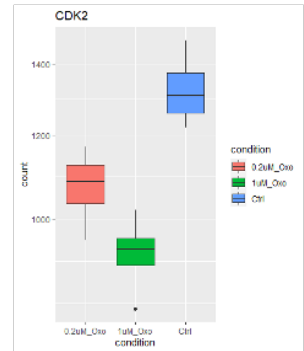
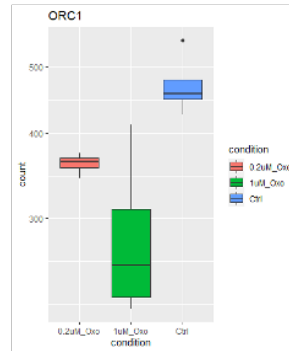
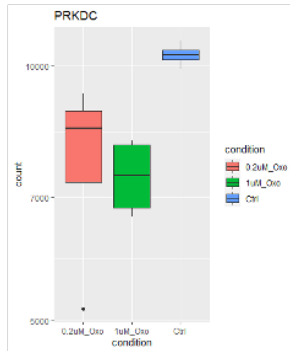
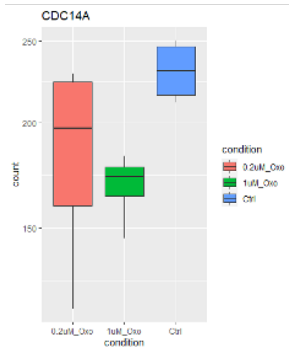
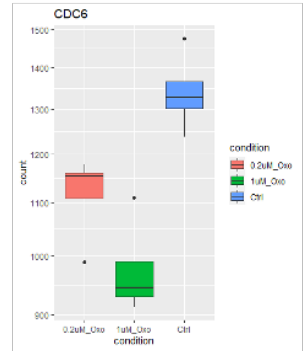
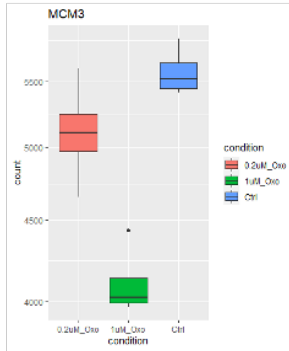
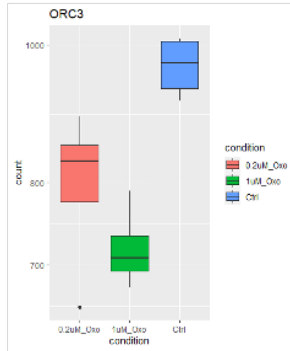
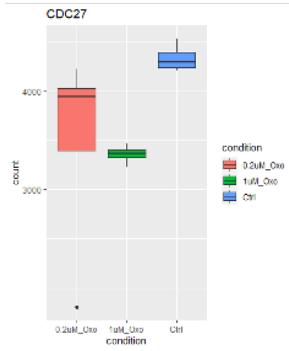


**Figure S3** Heat map generated from unsupervised clustering of genes from gene set of 'DNA Replication' (Reactome Pathway Database) of 0.2  $\mu$ M and 1  $\mu$ M 5Z-7-oxozeanol treated TIME cells and normal controls.





# KEGG\_Cell Cycle: Control vs. 1 $\mu$ M Oxo





## KEGG\_Cell Cycle: Control vs. 1 $\mu$ M Oxo



**Figure S4 (A)** Circular plot of KEGG pathway (cell cycle and DNA replication) enrichment analysis. **(B)** Bar charts show the normalized read count of each gene in the gene set of ‘Cell Cycle’ identified by GSEA study in TIME cells treated with 1  $\mu$ M 5Z-7-oxozeaenol. **(C)** Bar charts show the normalized read count of each gene in the gene set of ‘DNA Replication’ identified by GSEA study in TIME cells treated with 1  $\mu$ M 5Z-7-oxozeaenol.

**Figure S5**

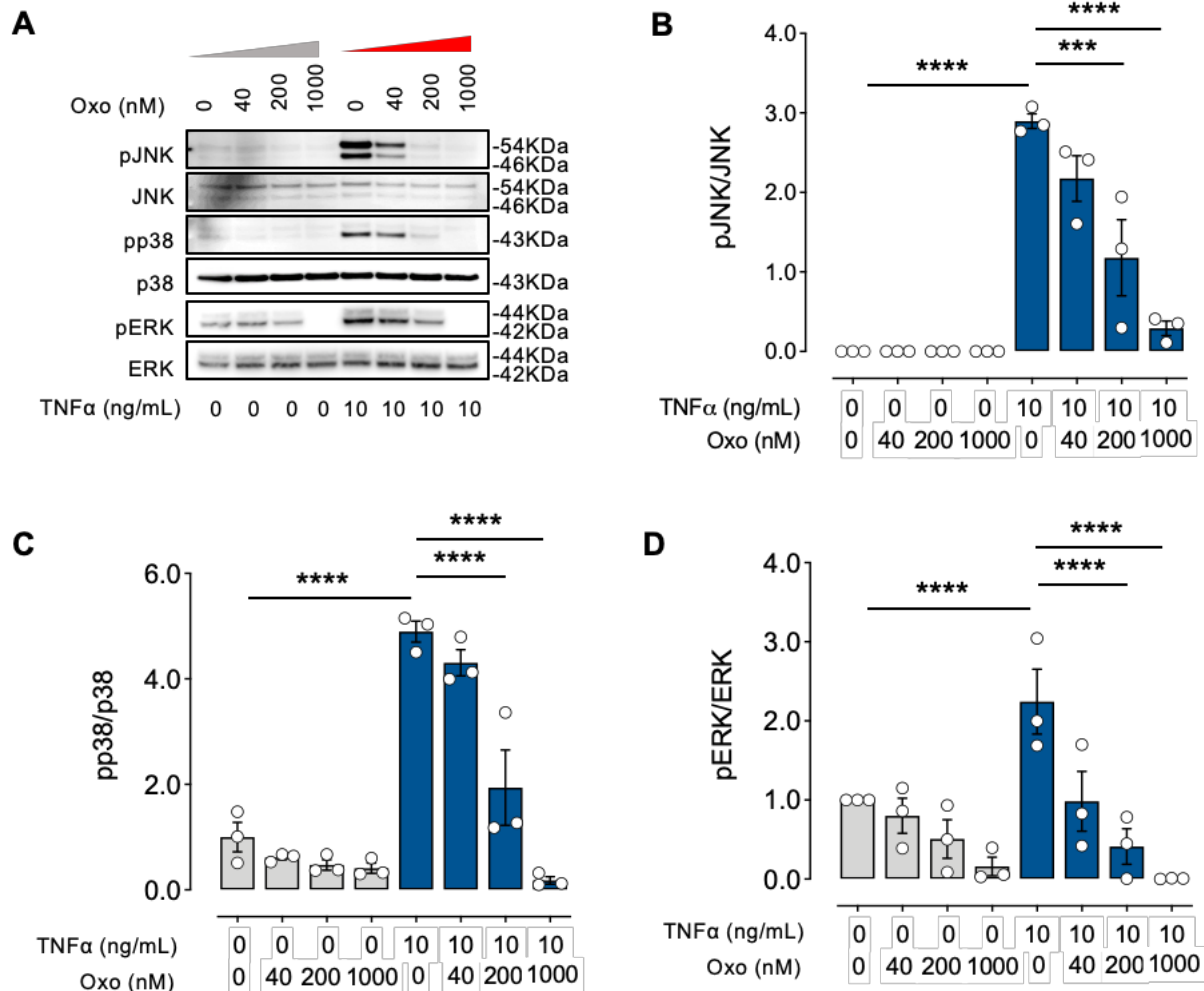


**Figure S5 5Z-7-oxozeaenol suppresses inflammatory cytokine-mediated MAPK signaling.** (A) Western blot characterization of the TNF $\alpha$ -induced phosphorylation of JNK, p38, and ERK proteins in TIME cell stimulated by TNF $\alpha$  (10 ng/ml) for 10 minutes. (B-D) Phosphorylation of JNK, p38, and ERK proteins in MAPK signaling was decreased in cells treated with 5Z-7-oxozeaenol in a dose-dependent manner (n = 3 from three experiments). Statistical analysis was conducted by one-way ANOVA and Tukey's multiple comparison test. \*\*\* $P < 0.001$ , \*\*\*\* $P < 0.0001$ .

**Figure S6**



**Figure S6 Characterization of gelatin nanoparticle-encapsulated 5Z-7-oxozeaenol.** Representative images from dynamic light scattering (DLS) analysis revealed the particle polydispersity index (PDI), size, and zeta potential of GNP and GNP-Oxo particles. Each sample was tested in triplicates, shown as red, green, and blue lines.

**Figure S7**

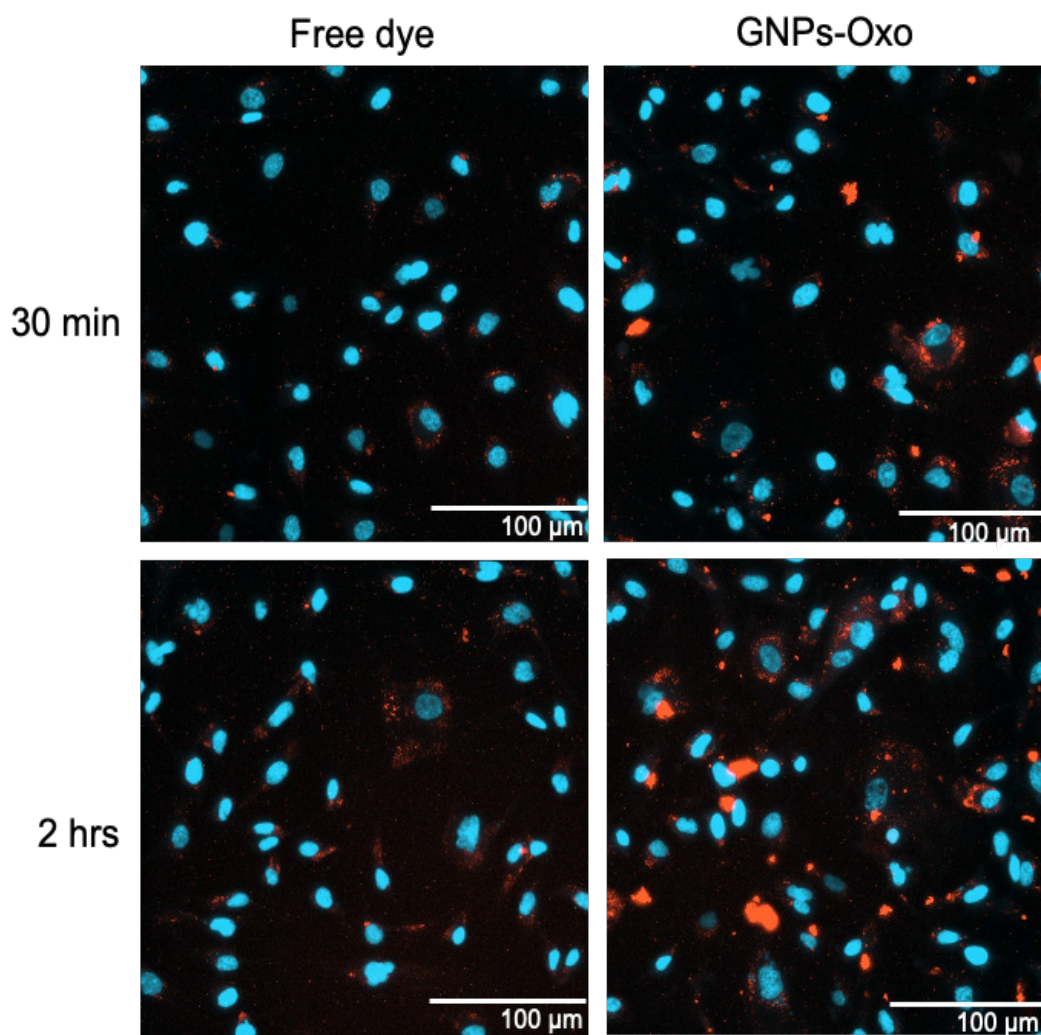


**Figure S7 The distribution of nanoparticles conjugated with fluorescence dye (TAMRA) in HUVECs.** Cells displayed clearer staining in the cytoplasm and even near nucleus 30 minutes post-treatment with GNPs-Oxo and much more staining intracellularly 2 hours post-treatment with GNPs-Oxo. Red and blue represent fluorescence dye (TAMRA) and DAPI staining, respectively. Scale bar: 100 μm.

**Figure S8**

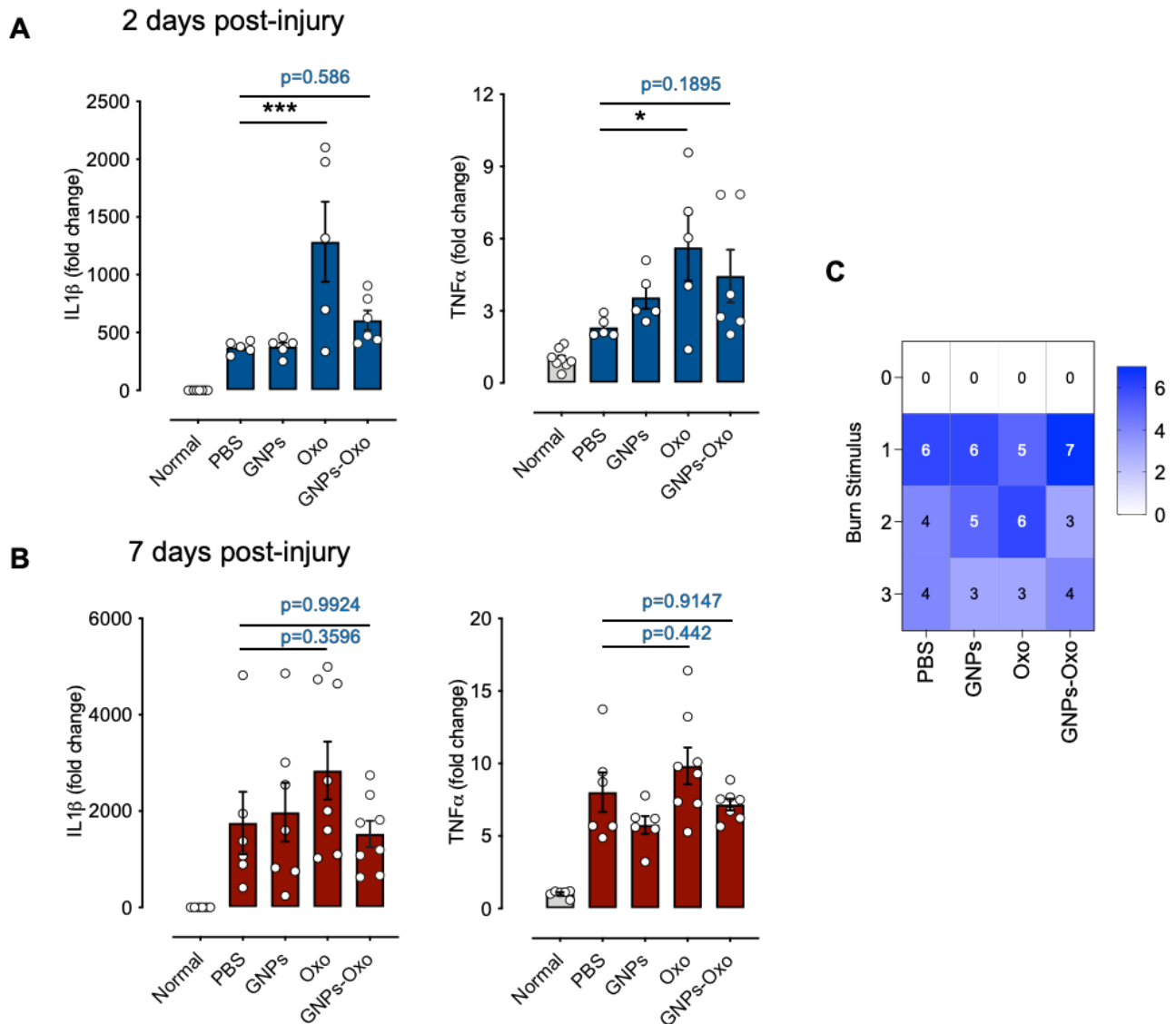


**Figure S8** Gelatin nanoparticle-encapsulated 5Z-7-oxozeaenol reduces inflammatory responses developed in the mouse model of CoNV. **(A and B)** IL-1 $\beta$  and TNF $\alpha$  expression was significantly increased 2- and 7-days post-injury in mice, while GNP-Oxo treatment moderately reduced the IL-1 $\beta$  and TNF $\alpha$  expression (n = 5-8 corneas per treatment group). **(C)** Quantitative analysis of corneal blisters after chemical cauterization showed no difference among groups (see methods about the grading; n = 14 animals per treatment group from three experiments). Statistical analysis was conducted by one-way ANOVA and Tukey's multiple comparison test. \* $P < 0.05$ , \*\*\* $P < 0.001$ .



Uncropped WB images  
Figure 3A

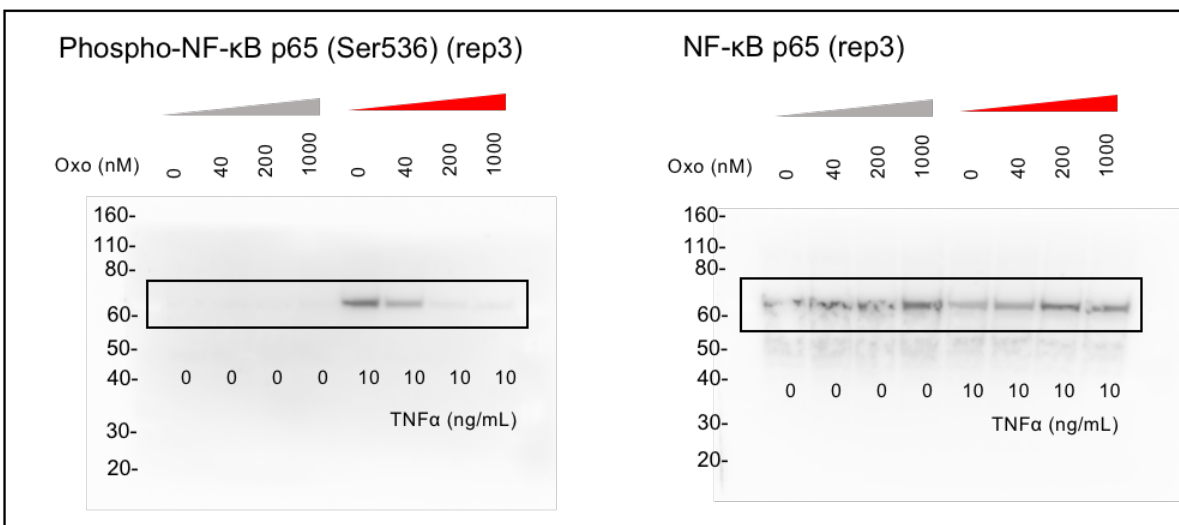
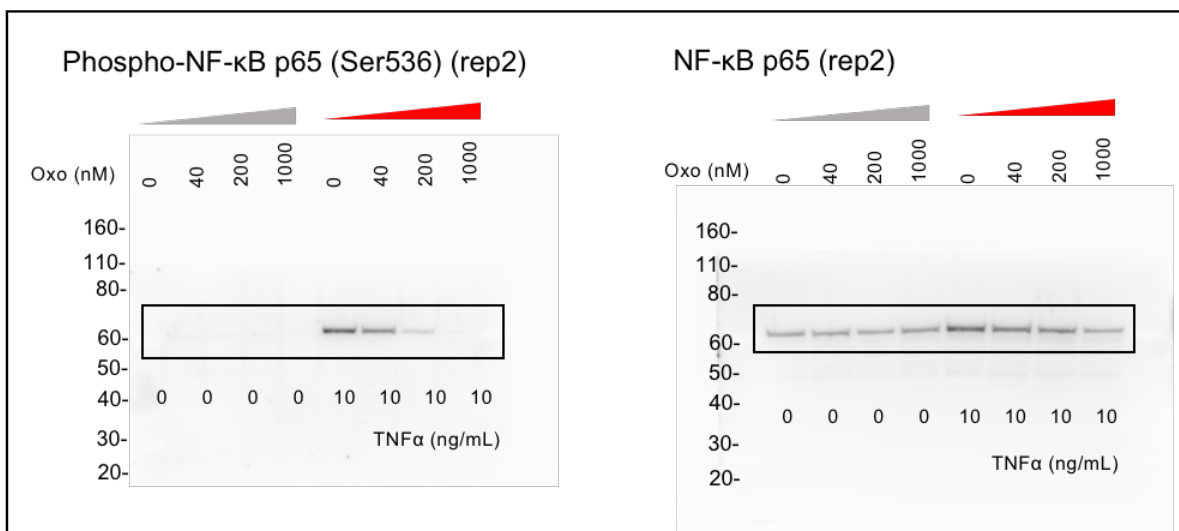
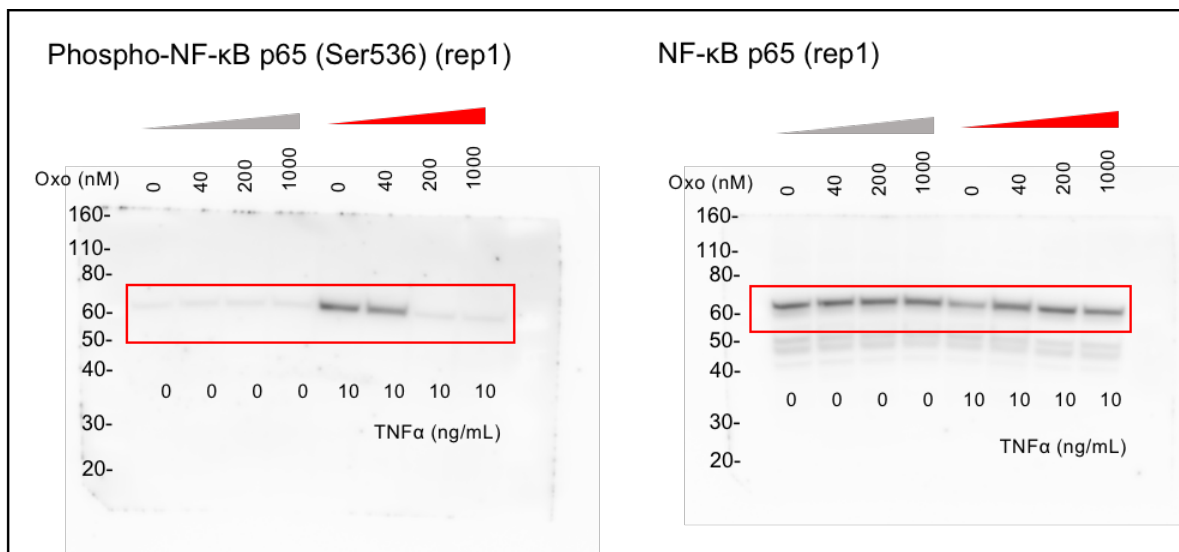


**Figure 3A**

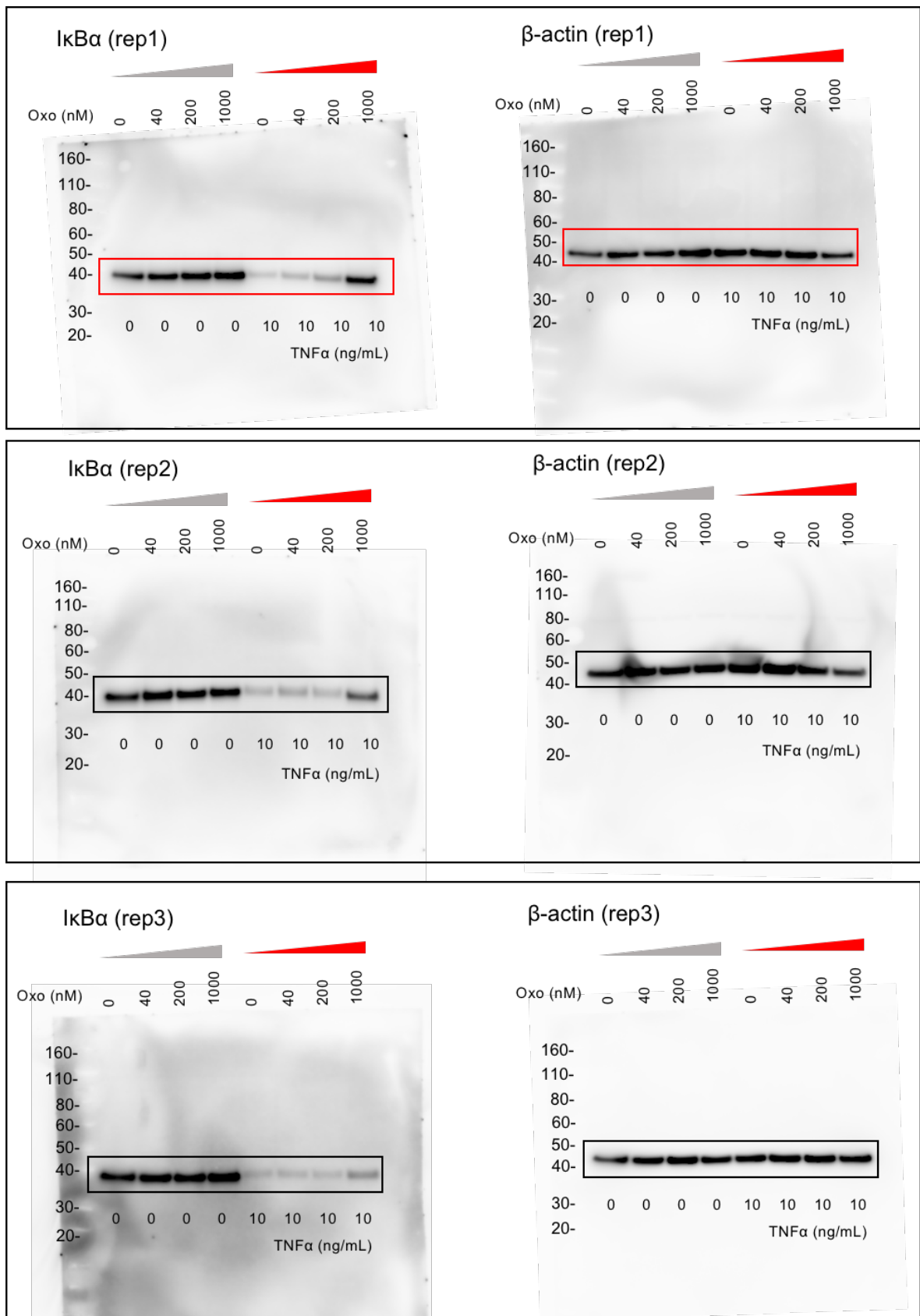


Figure S5A

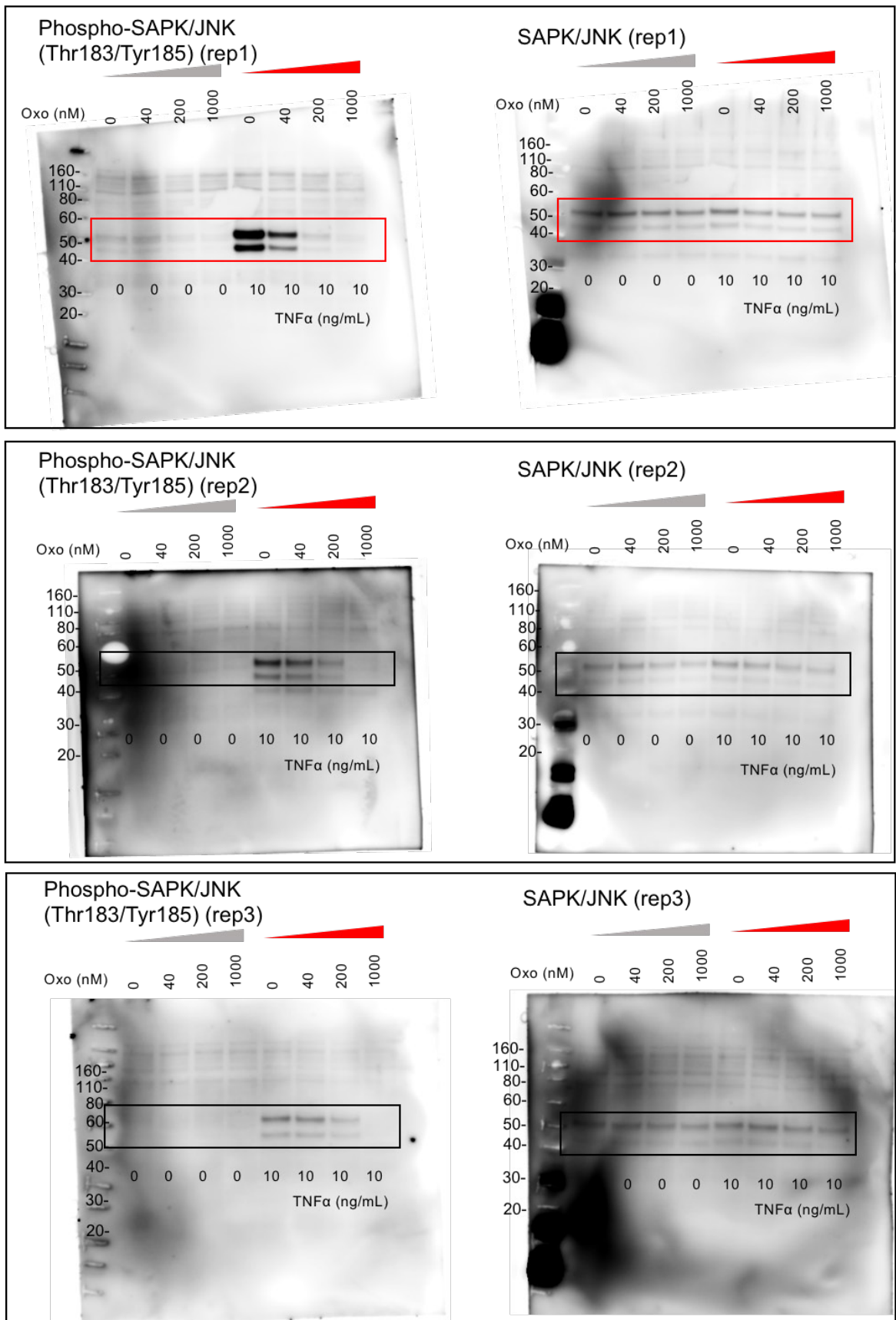


Figure S5A

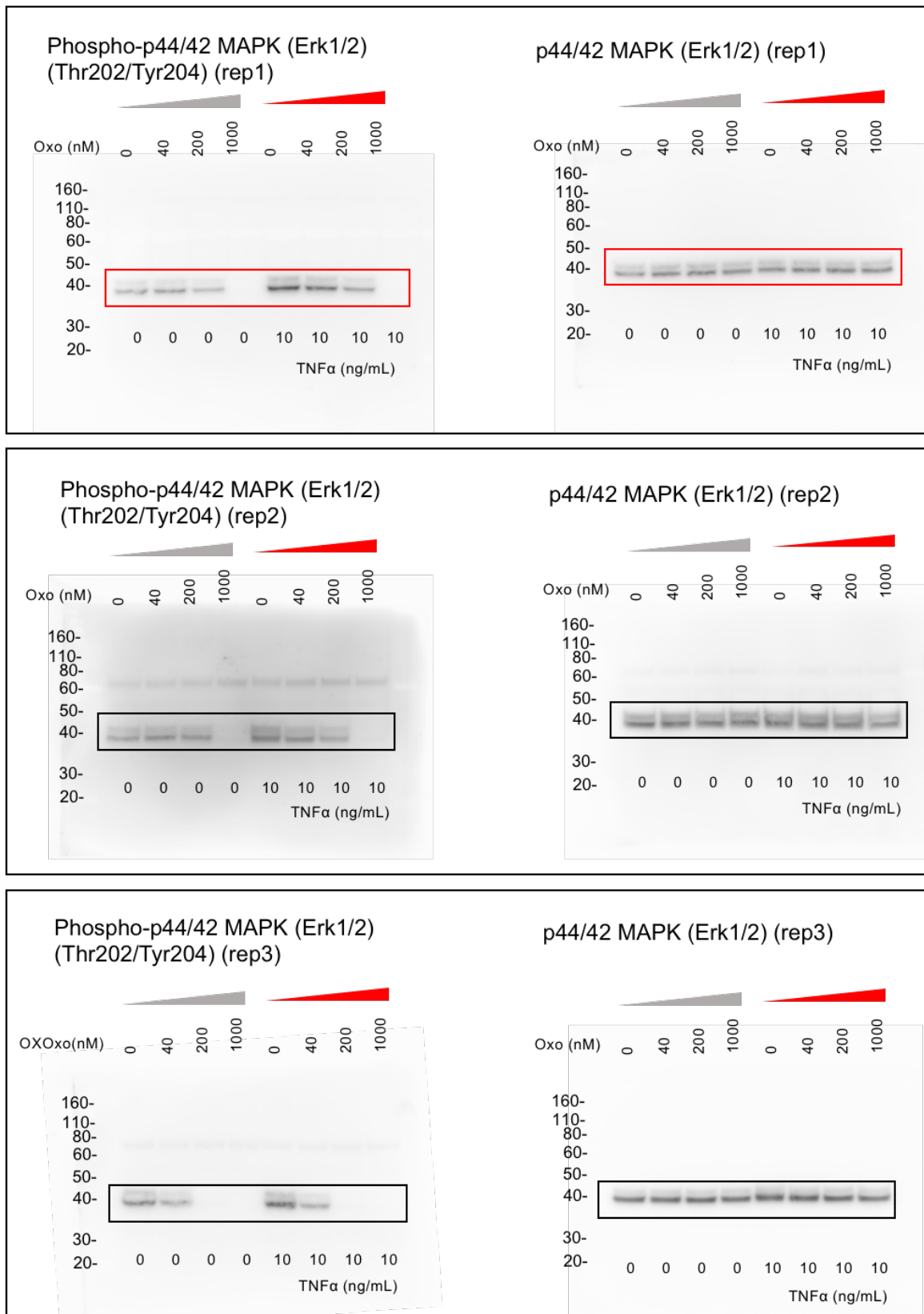


Figure S5A

